Supplemental Document

Biomedical Optics EXPRESS

Light-sheet fluorescence microscopy for the *in vivo* study of microtubule dynamics in the zebrafish embryo: supplement

MATTEO BERNARDELLO,[1,2] MARIA MARSAL,[1,2] EMILIO J. GUALDA,[1,2] AND PABLO LOZA-ALVAREZ[1,*]

[1] *ICFO-Institut de Ciencies Fotoniques, The Barcelona Institute of Science and Technology, Castelldefels, 08860, Spain*
[2] *equal contribution*
[*] *pablo.loza@icfo.eu*

Supplement DOI: https://doi.org/10.6084/m9.figshare.16458405

Parent Article DOI: https://doi.org/10.1364/BOE.438402

Light-Sheet Fluorescence Microscopy for the *in vivo* study of microtubule dynamics in the zebrafish embryo: supplemental document

Supplement 1

1. Supplementary Methods

1.1 Zebrafish embryos breeding and imaging

TG(XlEef1a1:dclk2-GFP) [1] (noted as dclk2-GFP) females were crossed with AB WT males and the embryos collected and maintained in E3 medium, and staged as in [2].

In order to be mounted in the first LSFM setup (shown in Fig. 1A-B), one embryo was transferred to a petri-dish and left in a small drop of water. A 1.5% low melting agarose solution in E3, previously heated up to 70°, was left to cool down until approx. 40°. While still liquid, the lmpa solution was poured in the petri-dish to completely cover the embryo. The lmpa solution and the embryo were aspired within a glass capillary through a plunger. After solidification, the lmpa cylinder was extruded and cut until approximately 1 mm from the embryo position. Other 5 mm, in which the embryo was placed, were extruded from the glass capillary. The microscope xyz stage permits the insertion and fixation of the glass capillary in such a way that the extruded agarose falls within the FoV of the objective. Note that the embryo was not dechorionated, i.e. no mechanical constriction was induced by the 1.5% lmpa cylinder. The incubation chamber was filled with 17 ml of E3 medium.

In the second LSFM setup (shown in Fig 1C-D), a fluidic circuit (1.5 m long) composed of a FEP tube filled with E3 medium crosses the incubation chamber at 45° with respect to the illumination objectives, on the horizontal plane. On one side of the FEP tube (1mm ID) the zebrafish embryo can be inserted, and the programmable syringe pump connected to the opposite end of the tube is used to flow the specimen until it reaches the FoV of the vertically positioned detection objective. Once here, the scanning through the horizontal light sheet(s) is performed by the motorized vertical translation of the entire imaging chamber. The chamber is also filled with E3 medium. Note that the embryo is not dechorionated and that there is no use of agarose. The pump blocks the flow and prevents the sample from moving during the acquisition of the images. The embryo is mounted only by its insertion in the fluidic circuit, without the need to wait for agarose solidification, which facilitates the entire procedure and greatly reduces the time required. The sample can be also easily retrieved from the setup.

In both setups two illumination objectives are employed to implement an alternated double excitation scheme, i.e. generating one light sheet on each side of the embryo sequentially. Due to the large size of the zebrafish embryo, a simultaneous illumination scheme would create heavy artefacts derived from the inefficient excitation of the second half of the sample. The alternate illumination is implemented by blocking sequentially the beam of one excitation arm, through a 3D printed bar inserted in each illumination arm and moved by a servo motor.

1.2 Microscopes' resolution

In this work different detection objectives and tube lenses have been used, and the corresponding parameters have been resumed in Table S1. The theoretical lateral resolutions for each configuration are represented by the Full Width Half Maximum (FWHM) of the theoretical PSF, obtained through the plugin "PSF Generator" in FIJI. The axial resolution is instead equal to the FWHM of the light-sheet diameter, measured to be about 4.5 μm.

Note that the anisotropy of the 3D resolution does not affect the results of the analysis. The "local analysis" is performed on the maximum intensity projection images, where only the lateral resolution is considered. In the "global analysis", the positions of the circular ROIs are

calculated mathematically through spherical coordinates, i.e. independently from the actual resolution of the setup.

Table S1. The detection parameters obtained through the different configuration

Detection objective	Tube lens focal length [mm]	Total magnification	Pixel size [µm]	PSF theoretical lateral FWHM [µm]
Nikon 10x, 0.3NA water	200	10x	0.65	1.45
Nikon 10x, 0.3NA water	300	15x	0.43	1.10
Olympus 20x, 0.5NA water	200	22.2x	0.29	0.72
Olympus 20x, 0.5NA water	300	33.3x	0.20	0.60

1.3 Local analysis

Being the embryos mounted within their chorion, they are not constricted by any mounting medium, and can move. Particularly, the dividing cells can change position. Therefore, the FIJI plugin "Manual Tracking with Trackmate" [3] was used to manually track the moving cells/YSNs associated with a particular microtubule branch of the yolk cell, and a region of the branch itself. The obtained mean intensity graphs vs time calculated over the adopted ROIs (as shown in Fig. 3J and Fig. 3K), contain the information related to the cell cycle and to yolk's MT density. The analysis was performed on the maximum intensity projections of the z-stack over time. The diameter of the tracking ROIs was equivalent to 52 µm, and the tracks with the mean intensities were exported to CSV files.

1.4 Blastoderm margin analysis

A threshold was applied to the maximum intensity projection over time, to obtain the blastoderm shape in white over a black background. This allows the measurement to be independent of the cell's intensity variation over time. Perpendicular to the AV axis, a line ROI was drawn with FIJI and the intensity profile over time (showed in Fig. 3L) exported as CSV file.

1.5 Global analysis

Custom-made MATLAB scripts were developed to analyze the mean intensity of a 50 µm ROI traveling over the surface of a sphere modeling the embryo's yolk. From the acquired 3D images, the lateral and depth positions of the center of the yolk and of the vegetal pole were retrieved, and given as input to the software. Connecting those points, the direction of the animal-vegetal axis (AV axis) and the diameter of the yolk were calculated. The 3D coordinate system of the images (x as width, y as height, z as depth) was translated in the center of the sphere and rotated so that the z-axis lays on the AV axis. Based on this, the spherical coordinates of the sphere's meridians (defined by having the same azimuth coordinate) and parallels (defined by having the same elevation coordinate) were calculated and back-projected onto the 2D coordinate system of the images' maximum intensity projection. Next, a 50 µm ROI was allowed to travel over the meridians, at the different elevation angles, to follow the path of the MOWs, i.e. from the blastoderm margin towards the vegetal pole, over the yolk's surface. For every position and movie's frame, the mean intensity of the ROI was calculated. By plotting as kymograph, the normalized intensities over time at the different elevation angles of the same meridian, the signal's valleys marking the passage and propagation of the MOW are visible, and their speed is calculated from the images in degree/min by linear fitting. This was done for all the calculated meridians. From the angular speed in degree/min (denoted as w), linear velocities in µm/min (denoted as v) were calculated using the formula $v = r \cdot (w \cdot \pi) / 180$, where r is the yolk radius calculated for the specific embryo under examination. The kymograph obtained from the normalized intensities over time at the different azimuth angles of the same

parallel, permits to analyze the symmetry with respect to the AV axis of the MOWs' passage at the given latitude. This was done for each calculated parallel. The same algorithm has been used to model the blastoderm as a (hemi)sphere, and visualize the cells' division waves from the animal pole to the blastoderm margin. To load the images into the MATLAB console and for some graphical representation, ready MATLAB functions were downloaded from the MATLAB Central File Exchange [4–6].

1.6 Last MOW and last YSN division analysis

To evaluate the possibility that the last YSN division coincides temporally with the last MOW initiation, we used the "Manual Tracking with Trackmate" FIJI plugin in the 3D stack over time of the embryo under analysis to track the eYSN cycle. The eYSN were tracked over time in the 3D stacks and not in the maximum intensity projections since, in those images, with the onset of epiboly, the blastoderm would cover the YSL and block our view on the eYSN. The mean intensity of the tracks reflects the cycle of the eYSN, enabling the last divisions to be detected and permitting the post-mitotic nuclei to be followed for an additional time to ensure that no further division occurs. Only embryos for which the movie was long enough to ensure that the last YSN division was visible were taken into consideration and at least 3 YSNs/embryo were tracked. The tracking ROI had a diameter of 19 µm and the tracks with the intensity profiles were exported to a CSV file. The temporal information regarding the last MOW initiation was obtained either by detecting the mean intensity over time (through the FIJI z-profiler) of a ROI of 19 µm over the maximum intensity projection image of a microtubule branch, or from the previous local analysis. Its intensity profile was exported to a CSV file. The analysis was performed in six different embryos, following three YSNs per embryo, for at least 60 minutes after the last detected division.

1.7 Intensities plots

All the outputs generated from the different analysis containing the mean intensities either as text or CSV files, were imported to MATLAB, normalized, and plotted. Conclusions on the timing of the cell/YSNs divisions and MOW passages (correctness of the peak/valley position) were also checked by visual inspection of the related images.

1.8 Statistical analysis

To evaluate statistical significance, the software GraphPad Prism 9 was used. To compare the measures of cell/YSN mitosis periodicities between the three groups (defined by the experimental temperature) a Kruskal-Wallis test was performed, and p-values were evaluated with Dunn's multiple comparison test. The same approach was used to compare the measures of MOWs' initiation periodicities between the three groups. Two tailed p-values between the periodicities of cell/YSN divisions and MOWs' initiations at the same experimental temperature were evaluated through Mann-Whitney tests.

1.9 Immunostaining of WT embryos

Fixation and immunostaining procedures were obtained through an adaptation of the protocol described in [7]. Wild Type (WT) embryos were dechorionated and fixed in MT assembly buffer (80 mM KPIPES (pH 6.5), 5 mM EGTA, 1 mM MgCl2, 3.7% formaldehyde, 0.25% glutaraldehyde, 0.5 uM taxol, and 0.2% TritonX-100) for 6 hours at room temperature. After that, they were dehydrated and kept in methanol for different days at -20°C. Re-hydration was achieved through several washing in PBS with 0.1% NP40. After incubation in 100mM NaBH4 in PBS for up to 16 hours at room temperature, embryos were washed in tris buffered saline (TBS), and subsequently the blocking solution (2% BSA in TBS) was applied at room temperature for 30 minutes. Following, incubation of the embryos with β-tubulin primary antibody in blocking solution was performed at 4ºC, overnight. Embryos were then washed 5

times in TBS and incubated at room temperature with secondary antibody in blocking solution for 3 hours. Subsequently, after 4 washes in TBS, they were ready to be imaged. The mouse anti-β-tubulin antibody (E7, Developmental Studies Hybridoma Bank, DSHB) was used at 1:200, while the secondary antibody was in-house conjugated [8] to the Abberior STAR 635P fluorophore (Sigma) and used at 8ug/ml.

1.10 Photobleaching analysis

Visually, the images of all embryos except one did not presented relevant photobleaching, and the analysis here developed to detect the microtubule dynamics was performed on the raw data, i.e. without applying intensity correction strategies. The images of the only embryo affected by non-negligible photobleaching were corrected through the FIJI plugin "Bleach Correction" through an exponential fit. This photobleaching was caused by an imperfection present in the detection arm, which was later noticed and corrected.

Through FIJI, we also examined the mean intensity of a ROI positioned over the yolk region covered by microtubules in the maximum intensity projection, over time for the various embryos. After retrieving the mean intensity traces, we performed an exponential fitting. From the fits that showed an $R^2 > 0.75$ (meaning they are a good representation of the photobleaching decay), the decay constant λ was extrapolated, which represents the speed of the signal's loss. Its reciprocal, called "time constant" $\tau = 1/\lambda$, represents the time needed for the signal to show a decay of $1/e \approx 37\%$ from the initial value. The smaller the time constant, the higher the photobleaching effect.

We only detected a high photobleaching effect (τ =2.3 hours) for the previously mentioned embryo, that was later computationally corrected. Another trace showed a higher time constant (τ=6.2 hours), while all the other traces showed τ > 40 hours, i.e. the photobleaching was negligible for the duration of the imaging here discussed (ranging from a minimum of 1 to a maximum of 12 hours).

2. Supplementary figures and videos

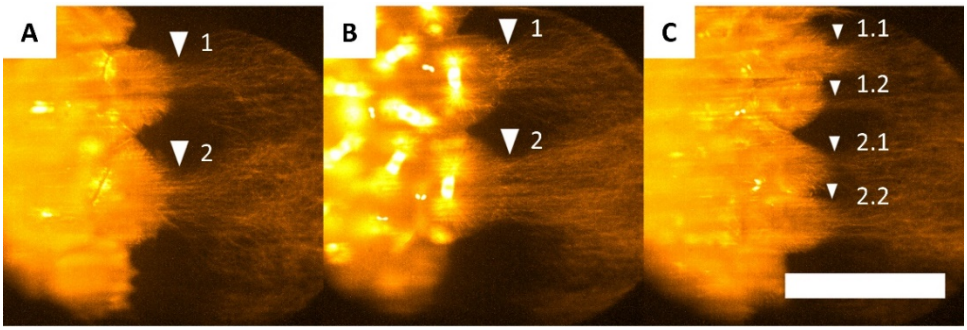

Supplementary Fig. S1: branching nature of the eMTN visualized in live dclk2-GFP. (A) Two branches emerge from the blastomeres (arrowheads) and (B) upon mitosis, (C) they divide into two sub-branches each (arrowheads). Scalebar 50 µm.

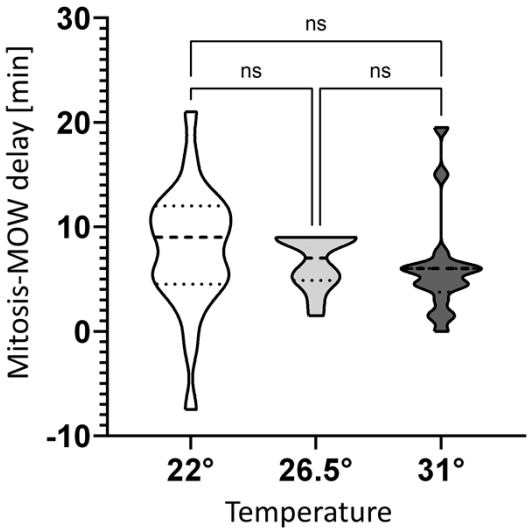

Supplementary Fig. S1: Violin plots showing the distribution of the delays between the mitotic event and the corresponding MOW initiation respect to the change of the developing temperature. The graph was generated in GraphPad Prism 9, and the significance was evaluated through a Kruskal-Wallis test.

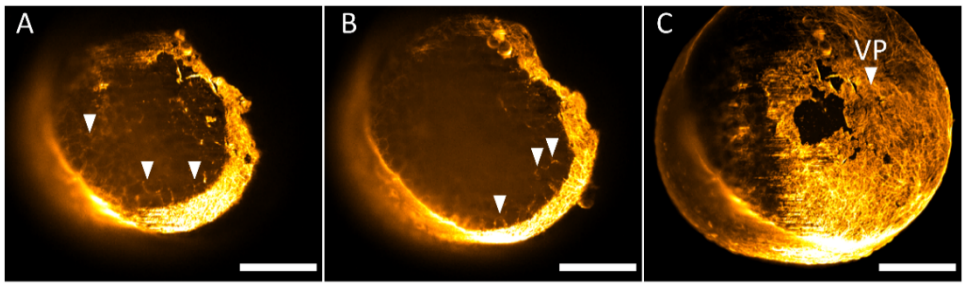

Supplementary Fig. S3: (A-B) Maximum intensity projection performed on two set of slices relative to the interior part of the yolk for a WT fixed and immunostained (β-tubulin) embryo. Fluorescent signal appears from the iMTN below the YCL, surrounding the lipid yolk granules (arrowheads). (C) Maximum intensity projection of all the slices to show the entire imaged volume as reference, with approximated position of the vegetal pole (VP and arrowhead). The yolk in (C) appears slightly damaged, possibly due to mechanical rupture after the immunostaining protocol. Scalebars 200 µm.

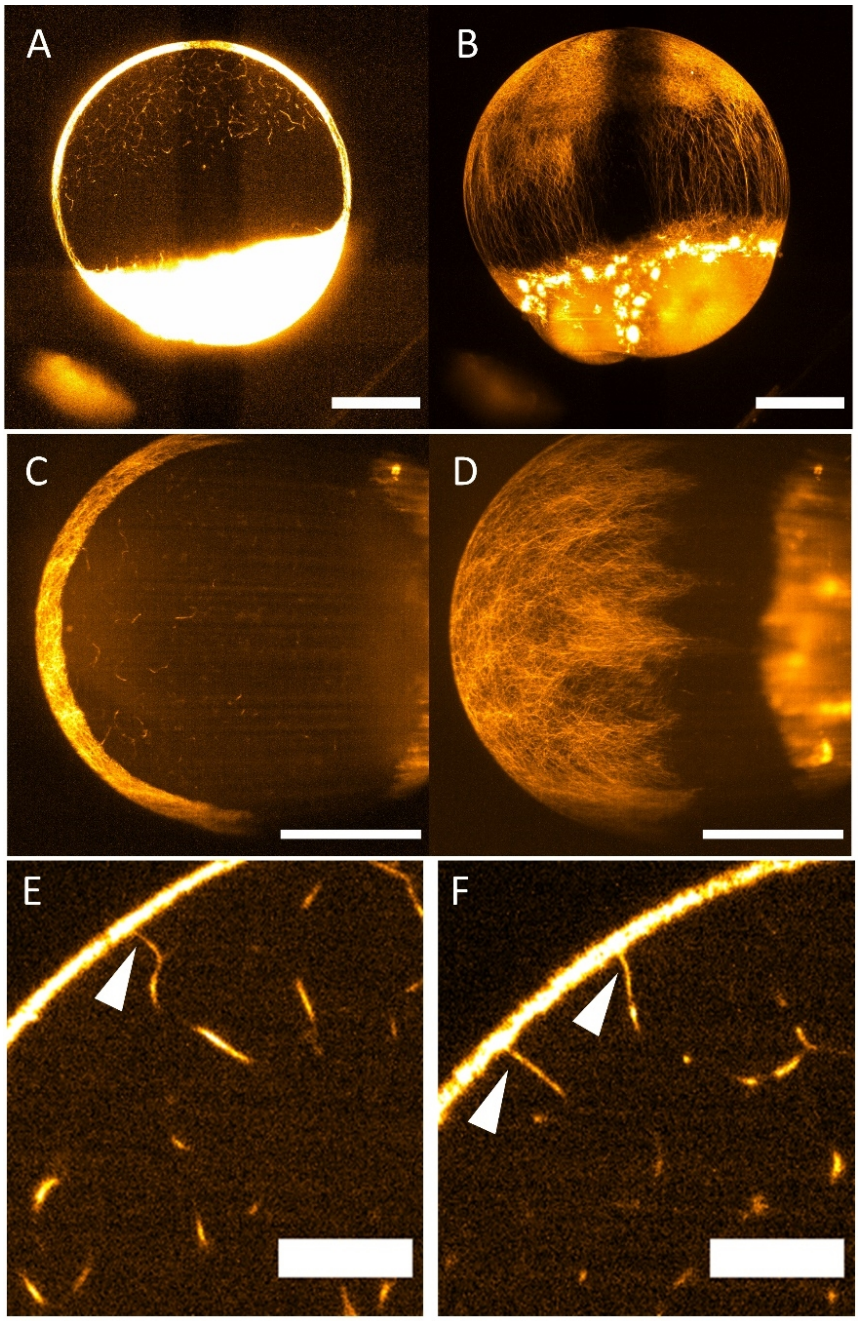

Supplementary Fig. S4: The maximum intensity projection performed on images relative to the interior part of the yolk for a non-fertilized egg (A) and an embryo at cleavage stage (C) reveals the presence of the iMTN. The eMTN visualized through the maximum intensity projection performed on the whole z-stack for the same eggs is also provided (B, D). Scale bars 200 µm. (E-F) Single slice images showing in live dclk2-GFP the connections between the eMTN and the iMTN (arrowheads) before (E) and after (F) a MOW passage. The displayed area is the same as that shown in Figure 6B-D. Scalebars 50 µm. All images relative to dclk2-GFP eggs.

Visualization 1: LSFM imaging of a dclk2-GFP embryo (Vegetal view). Two MOWs are crossing the yolk over the YCL in a belt-like fashion, bundling the eMTN, and closing concentrically at the vegetal pole. Scale bar 100 µm. Central black region is due to the LS bending caused by the curvature of the sample.

Visualization 2: LSFM imaging of a dclk2-GFP embryo at blastula stages (Lateral view). Multiple MOWs are passing over the YCL from the blastoderm margin toward the vegetal pole, bundling the eMTN. Animal pole at top right, vegetal pole at bottom left. Scale bar 200 µm.

Visualization 3: LSFM imaging of a dclk2-GFP embryo from cleavage until bud stages (Lateral view). Several MOWs are shown, but no MOWs are visible during epiboly. Animal pole at top right, vegetal pole at bottom left. Scale bar 200 µm.

Visualization 4: Video formed by three movies on the same area of a dclk2-GFP embryo. The z-stack (from 00:00 to 00:19) starts from the interior of the yolk and continues towards the surface, where an eYSN is placed. It shows an internal MT bundle (arrowhead) connected to the eYSN. A 3D rotating projection of the same area (from 00:20 to 00:23) shows the extension of the same MT bundle towards the interior of the yolk, and again its connection to the eYSN (arrowhead). A resliced view (YZ) of the same area (from 00:24 to 00:30) shows the evolution of the connection between the internal MT bundle and the eYSN versus time. The connections (arrowheads) are lost upon eYSN mitosis and reform with the resulting nuclei. Orange HOT colormap is used to ease visualization of the internal MT bundle. Time stamp in minutes : seconds. Scale bar 50 µm.

Visualization 5: Video formed by three movies in the same area of a dclk2-GFP embryo. The z-stack (from 00:00 to 00:09) shows another internal MT bundle (arrowhead) connected to an eYSN. A 3D rotating projection of the same area (from 00:10 to 00:12) shows the extension of the same MT bundle toward the interior of the yolk, and again its connection to the eYSN (arrowhead). The same area (from 00:13 to 00:18), visualized through a maximum intensity projection over 20 µm in depth, shows the evolution of the connection between the internal MT bundles and the eYSN versus time. The connections (arrowheads) are lost upon eYSN mitosis and reform with the resulting nuclei. Orange HOT colormap is used to ease visualization of the internal MT bundle. Time stamp in minutes : seconds. Scale bar 50 µm.

Visualization 6: Maximum intensity projection over 30 µm showing the section of the interior of the yolk. LSFM imaging of the dclk2-GFP embryo was performed from about sphere until bud stages. The iMTN is visible in the whole yolk and it is present also during epiboly. The embryo moves as it is not constricted by the mounting medium. Animal pole at top/top-right, vegetal pole at bottom/bottom-left. Time stamp in minutes : seconds. Scale bar 200 µm.

Visualization 7: Maximum intensity projection over 40 µm showing the section of the interior of the yolk, from LSFM imaging of a dclk2-GFP embryo (from 00:00 to 00:07). The connections between eMTN and iMTN are lost upon MOW passage, and reform afterwards. Scale bar 200 µm. A ROI is highlighted (from 00:08 to 00:12) to better visualize the connections' dynamics (arrowheads). Scale bar 50 µm. Orange HOT colormap is used to ease visualization of the iMTN.

References

1. L. D. Tran, H. Hino, H. Quach, S. Lim, A. Shindo, Y. Mimori-Kiyosue, M. Mione, N. Ueno, C. Winkler, M. Hibi, and K. Sampath, "Dynamic microtubules at the vegetal cortex predict the embryonic axis in zebrafish.," Development **139**(19), 3644–3652 (2012).

2. C. B. Kimmel, W. W. Ballard, S. R. Kimmel, B. Ullmann, and T. F. Schilling, "Stages of embryonic development of the zebrafish.," Dev. Dyn. an Off. Publ. Am. Assoc. Anat. **203**(3), 253–310 (1995).

3. J.-Y. Tinevez, N. Perry, J. Schindelin, G. M. Hoopes, G. D. Reynolds, E. Laplantine, S. Y. Bednarek, S. L. Shorte, and K. W. Eliceiri, "TrackMate: An open and extensible platform for single-particle tracking.," Methods **115**, 80–90 (2017).

4. Y. Tak, "Multipage TIFF stack,"

https://www.mathworks.com/matlabcentral/fileexchange/35684-multipage-tiff-stack.

5. D. Helmick, "varycolor," https://www.mathworks.com/matlabcentral/fileexchange/21050-varycolor.

6. T. Davis, "Arrow3," https://www.mathworks.com/matlabcentral/fileexchange/14056-arrow3.

7. J. Topczewski and L. Solnica-Krezel, "Cytoskeletal dynamics of the zebrafish embryo.," Methods Cell Biol. **59**, 205–226 (1999).

8. Š. Bálint, I. Verdeny Vilanova, Á. Sandoval Álvarez, and M. Lakadamyali, "Correlative live-cell and superresolution microscopy reveals cargo transport dynamics at microtubule intersections.," Proc. Natl. Acad. Sci. U. S. A. **110**(9), 3375–3380 (2013).